SCIENTIFIC REPORTS

OPEN

Dielectric meta-atom with tunable resonant frequency temperature coefficient

Lingling Wu[1], Xiaoqing Xi[1], Bo Li[2] & Ji Zhou[1]

In this paper, we present a proof-of-concept of a new approach to achieving tailored resonant frequency temperature coefficients in dielectric meta-atoms. The technique involves introducing a thermally expanding or contracting material joining the active high permittivity dielectric absorbers. Both simulation and experiment show that by careful design of the element size and appropriate choice of thermomechanical intermediate layer material, increased or decreased resonant frequency shift temperature sensitivity is possible. Once the active dielectric material is chosen, and a meta-atom design determined, we show the resonant frequency shift depends on the thermal expansion coefficient of the intermediate layer. This work demonstrates the feasibility of manipulating the blue or red shift of metamaterial devices by introducing temperature responsive intermediate layers into meta-atoms.

In the past decades, electromagnetic (EM) metamaterials[1–3] have attracted considerable enthusiasm of researchers because of their remarkable properties that could be applied to achieve abnormal permittivity or permeability[4–6], EM cloaking[7–9], perfect lensing[10, 11], tunable band-pass filters[12, 13], microwave couplers[14], absorbers[15] and other uses. Compared with resonant metallic elements, nonmetallic dielectric resonators show a lot of advantages in constructing metamaterials with isotropic electromagnetic responses and smaller conductive loss at high operating frequencies[16]. There are many forms of electric or magnetic resonance in dielectric materials[17, 18], such as ferroelectrics[19], negative permeability Mie resonance particles[20], ferromagnetic resonance in ferrites[21] and others. Among these, Mie resonance is a simple approach based on displacement currents[22–24]. The first order Mie resonance frequency f_1 is given by

$$f_1 = \frac{\theta_1 c}{2\pi r \sqrt{\varepsilon_2 \mu_2}} \tag{1}$$

where θ_1 is a constant close to π, c is the light velocity in vacuum, r is the radius of dielectric meta-atoms, ε_2 and μ_2 is the relative permittivity and permeability of the dielectric meta-atoms. For non-magnetic dielectric material, μ_2 is usually approximately equal to 1. As suggested by equation (1), once the size of the dielectric element is fixed, the frequency of the first order Mie resonance is decided by the relative permittivity of the dielectric material. The permittivity of many important dielectric materials such as $CaTiO_3$ are very sensitive to temperature[25, 26]. The frequency shift of the dielectric materials caused by temperature change is characterized by the temperature coefficient of resonant frequency (TCF), which is calculated by

$$\tau_f = -\left(\frac{1}{2} \tau_\varepsilon + \alpha_L \right) \tag{2}$$

where τ_f is the TCF, τ_ε is the temperature coefficient of permittivity, and α_L is the linear thermal expansion coefficient. Many investigations have manipulated τ_f to achieve desired blue or red shifts to fulfil the specific practical requirements. Several of these obtained tunable τ_f by mixing two of more opposite τ_f materials[27, 28], such as $MgTiO_3$-$CaTiO_3$[29] and $Ba(Zn,Nb)O_3$-$Ba(Zn,Ta)O_3$[30]. Unfortunately, the fabrication process of these composites is usually very complicated and involves high sintering temperature. Moreover, the component materials to be

[1]State Key Laboratory of New Ceramics and Fine Processing, School of Materials Science and Engineering, Tsinghua University, Beijing, 100084, China. [2]Advanced Materials Institute, Shenzhen Graduate School, Tsinghua University, Shenzhen, China. Correspondence and requests for materials should be addressed to J.Z. (email: zhouji@mail.tsinghua.edu.cn)
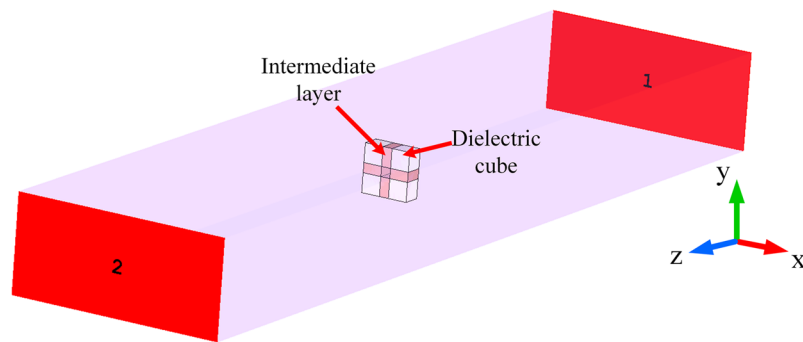
1

Figure 1. Schematic of the model meta-atom and test environment used in the simulation.

mixed together should be carefully selected to meet other requirement, such as high Q and proper value of ε, limiting their usability in meta-devices.

Therefore, a more universal approach to control TCF, applicable to most dielectric materials, is highly desirable. From equation (1), the TCF is closely connected with the coefficient of thermal expansion (CTE) of the material. This indicated to us that the TCF of materials could be manipulated by introducing a thermally responsive second component of suitable CTE into the design of the meta-atoms.

In recent years, tunable CTE artificial materials have been widely investigated, demonstrating negative-, positive- or near-zero CTEs[31–38], offering a simple and versatile route to manipulating the EM properties of metamaterials through thermal expansion or contraction. Therefore, by constructing the meta-atoms using both the high permittivity dielectric and a second material with a desired CTE, the TCF of the EM meta-devices could be manipulated. The second material would not have an absorption resonance, but would simply act to change the spacing between the active dielectric elements.

In this paper, we use low-cost and easily accessible thermally sensitive materials in a simple design. We introduce tailored CTE joints connecting separate blocks of high permittivity dielectric. The meta-atom then consists of a tiling of dielectric and thermomechanical materials. Through simulation and experimental result, we show that the effective TCF of the meta-atom is closely related to the CTE value of the expanding or contracting joints. We will call these joints the intermediate material or equivalently the intermediate layer. We believe that this approach could be broadly applied in EM device design using tailorable TCF to meet specific performance requirements. When temperature of such a device changes, the intermediate material will shrink or expand to either cancel or enhance the effects of the permittivity variation with temperature. Permittivity changes alone cause blue shifts in the resonance frequency with increasing temperature. Thermal expansion pushing the active elements apart also blue shifts the frequency. Contraction upon heating, a negative CTE, red shifts the frequency and can in principle cancel the permittivity-induced shift. The resonant frequency could then potentially be held stable. Alternately, with a positive CTE intermediate layer, it can be given a significant chirp upon heating.

Results

To demonstrate the feasibility of our proposed method, a meta-atom composed of four dielectric cubes and thermally variable intermediate layer is designed in this paper. To explore the relationship between the thermal expansion of the intermediate layer and the effective TCF of the meta-atom, we carried out simulation work using the Microwave Studio software package (CST Studio Suite 2016, Germany), on the model shown in Fig. 1. The dimensions of the rectangular vacuum box surrounded by a perfect conductor is 22.86 mm × 10.16 mm × 100 mm (EIA WR-90 waveguide), in which a single-mode with electric field E parallel to the y-axis from 8.2 GHz to 12.4 GHz (X-band) can be transmitted.

We firstly simulated the relationship between the width of intermediate layer and the first order resonant frequency of the meta-atom. The meta-atom was designed with four dielectric cubes with a cross-shaped intermediate layer with a constant permittivity of 2.3. To simplify the modeling and to match experiment, the dielectric cubes have a permittivity of 120.6 at room temperature ($CaTiO_3$ ceramic). The simulated result is shown in Fig. 2. The first order resonant frequency has a blue shift as the width of the intermediate layer increases from 0.4 to 1 mm.

Since the CTE of dielectric cubes is very small, we neglect the thermal expansion, and only consider the expansion of intermediate layer. The permittivity of $CaTiO_3$ ceramic decreases with increasing temperature in accordance with the Curie-Weisslaw, so the first resonant frequency will also have a blue shift when temperature increases, as shown in Fig. 3(a). During the simulation, the thermal expansion coefficient of the intermediate layer α_{in} is varied from $-7 \times 10^{-3} K^{-1}$ to $-1 \times 10^{-4} K^{-1}$ in steps of $1 \times 10^{-4} K^{-1}$, and the temperature increases from 305.5 K to 373.0 K in steps of 7.5 K. The simulated frequency range is from 10.0 GHz to 12.4 GHz to coincide with the experiment. From the simulation result, the effective TCF of the meta-atom is calculated and shown in Fig. 3(b). The effective TCF of the meta-atom has an approximately linear dependence on the thermal expansion of the intermediate layer, and it is close to zero at $\alpha_{in} = -6.35 \times 10^{-3} K^{-1}$. The scattering matrix transmission coefficient S_{21} is shown in Fig. 3(c) and (d) versus frequency at a range of temperatures. Figure 3(c) is the calculated S_{21} spectrum for the square array of four dielectric cubes alone, while in Fig. 3(d) the cubes are joined by an intermediate layer with $\alpha_{in} = -6.35 \times 10^{-3} K^{-1}$.

The experiment measures the frequency spectrum of the transmission parameter S_{21} of three meta-atom samples. The setup is illustrated in Fig. 4(a). The dielectric samples are 2 × 2 × 2 mm ceramic cubes of $CaTiO_3$ doped
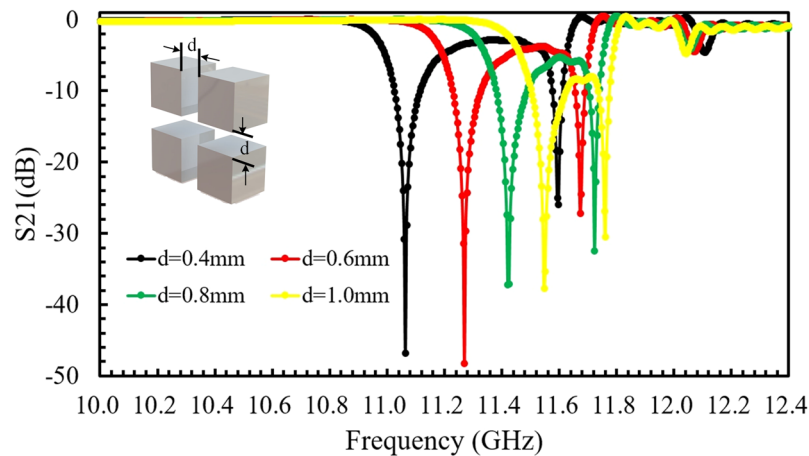
Figure 2. The relationship between the first order resonance frequency and the width of the intermediate layer.
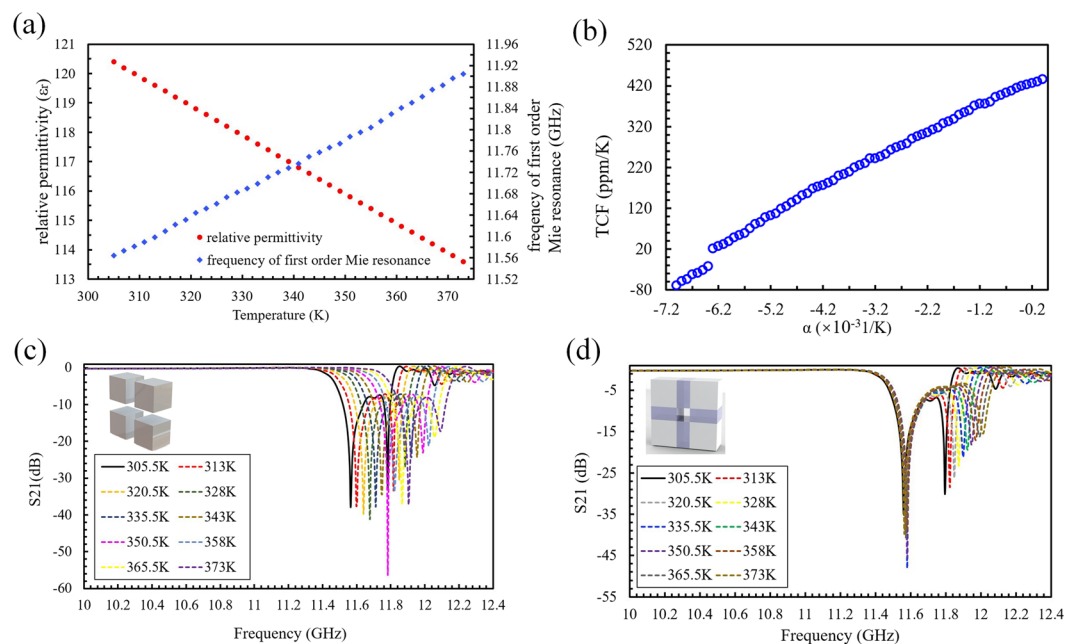

Figure 3. (**a**) Calculated relationship between the relative permittivity and temperature (red point curve) and the frequency of the first order Mie resonance and temperature (blue elliptical dot curve). (**b**) Calculated effective TCF of the meta-atom versus the thermal expansion coefficient of the intermediate layer. (**c,d**) The shift of the first order resonance frequency for the meta-atom (**c**) without elastic intermediate layer, and (**d**) with an intermediate layer ($\alpha_{in} = -6.35 \times 10^{-3}\,\mathrm{K}^{-1}$).

with 1 wt. % Zr_2O. At 305.5 K, the measured permittivity is 120.4 and the loss tangent is 0.007. For the first sample, we chose rubber as the intermediate layer, which has a large positive CTE of $2.42 \times 10^{-4}\,\mathrm{K}^{-1}$ and an initial width of 1 mm. Since natural materials with negative thermal expansion is rare and difficult to fabricate, we utilized heat-shrink tubing as the intermediate layer for the second sample to imitate the negative thermal expansion. The tubing has a diameter of 1.12 mm at 305.5 K, and 0.8 mm when the temperature is above 358.0 K. A third meta-atom sample with an intermediate layer of silica is also constructed. Silica has an extremely low thermal expansion of $5.3 \times 10^{-7}\,\mathrm{K}^{-1}$, which is much smaller than other materials, and the width of silica could be considered as constant. Therefore, the frequency shift of the third sample is measured as a comparative reference. The dielectric cubes were glued to the intermediate layers. Understanding that plastic or rubber components can absorb microwaves and contribute to the measured S_{21} values, and also damp the resonances, we repeated our experiments using smaller volumes of these materials on the second run. The reduced sizes in our second experiment were helpful, especially in the case of the shrink tubing. The photos of the fabricated meta-atom samples are shown in Fig. 5(e–g). This design effectively solved the problems of geometric distortion of the meta-atoms upon shrinkage of the tubing. However, there are still some discrepancies between the calculations and our measurements. These will be discussed below.
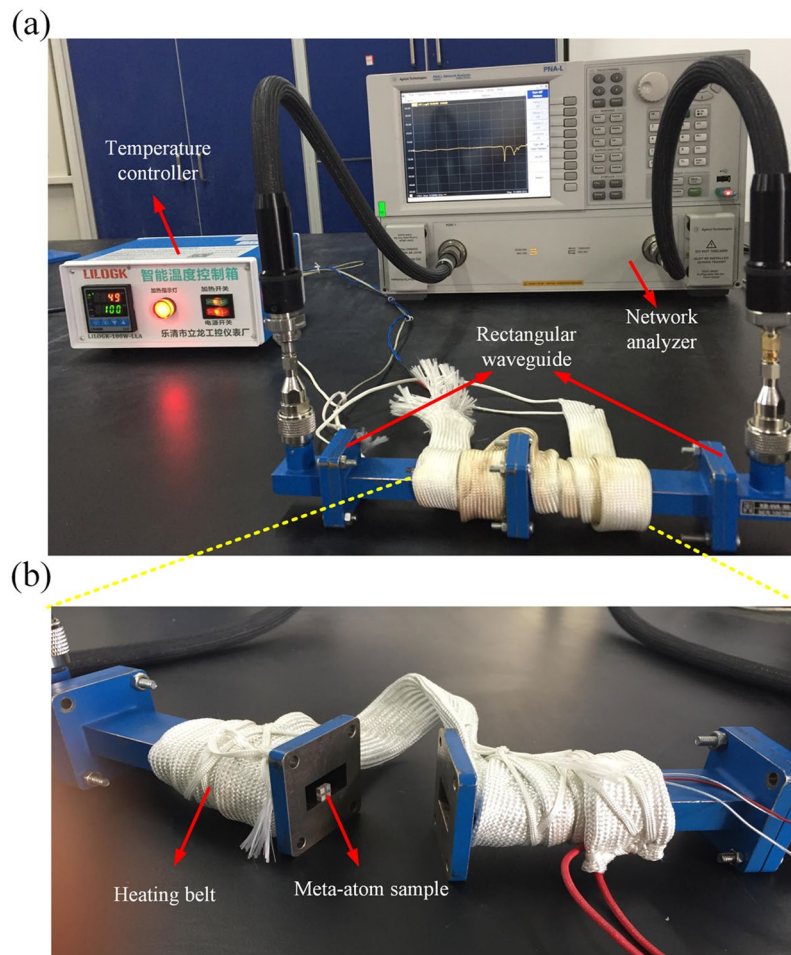
Figure 4. (**a**) The measurement setup. (**b**) The sample placed in the waveguide.

The experiment setup is composed of two WR-90 rectangular waveguides connected to the input and output of an Agilent PNA-LN5230C network analyzer, and a heating tape wound round the wave-guides and connected to an automatic temperature control heating device. During the measurements, all samples were placed in the same position in the waveguide, as shown in Fig. 4(b). As the simulation, the temperature was increased from 305.5 K to 373.0 K.

Discussions

The S_{21} spectra of the three samples at 305.5 K and 373.0 K are shown in Fig. 5(a–c). The resonance broadening and weakening observed in the silica-containing absorbers we attribute to size nonuniformity of the dielectric cubes. Additional broadening in the other two samples' spectra is attributable to the absorption in rubber and plastic. From the figures, we can calculate the effective TCF of the three meta-atoms, shown in Fig. 5(d). From left to right, these are $284.15 \times 10^{-6}\,K^{-1}$ for the sample with intermediate layer of heat shrink tubing, $454.56 \times 10^{-6}\,K^{-1}$ for silica, and $486.91 \times 10^{-6}\,K^{-1}$ for rubber. Clearly the rubber produced a greater blue shift in the resonance frequency than did the silica reference. The shrink tubing yielded a diminished blue shift, though it was significantly less of a decrease than the calculations indicated. Fabrication difficulties, in particular for the sample with shrink tubing, contributed to the discrepancies from calculation. Furthermore, although the permittivity of the intermediate layers is very low compared with the dielectric cubes, its slight change with temperature could also affect the measurement results. We also consider the temperature distribution in the samples may have been nonuniform, the plastic and rubber materials being better thermal insulators than the ceramic. Blue shifts caused by the permittivity changes in the ceramics may have arisen faster than blue or red shifts owing to thermal expansion or contraction. Efforts will be made to overcome this defect by improving the coefficient of thermal conductivity of the intermediate layer.

Although our design has some deficiencies at present, this work demonstrates the feasibility of tailoring the TCF of dielectric meta-atoms by introducing a thermally expanding or contracting intermediate layer. By appropriately designing the thermal expansion of the intermediate material, dielectric meta-atoms with tunable TCF could be achieved if suitable materials and high precision manufacturing process are available. Here, we have used $CaTiO_3$ ceramic cubes as the dielectric cubes, but this approach is not limited to dielectric meta-atoms. Enhanced or reduced TCF can be designed for other EM devices following a similar method.
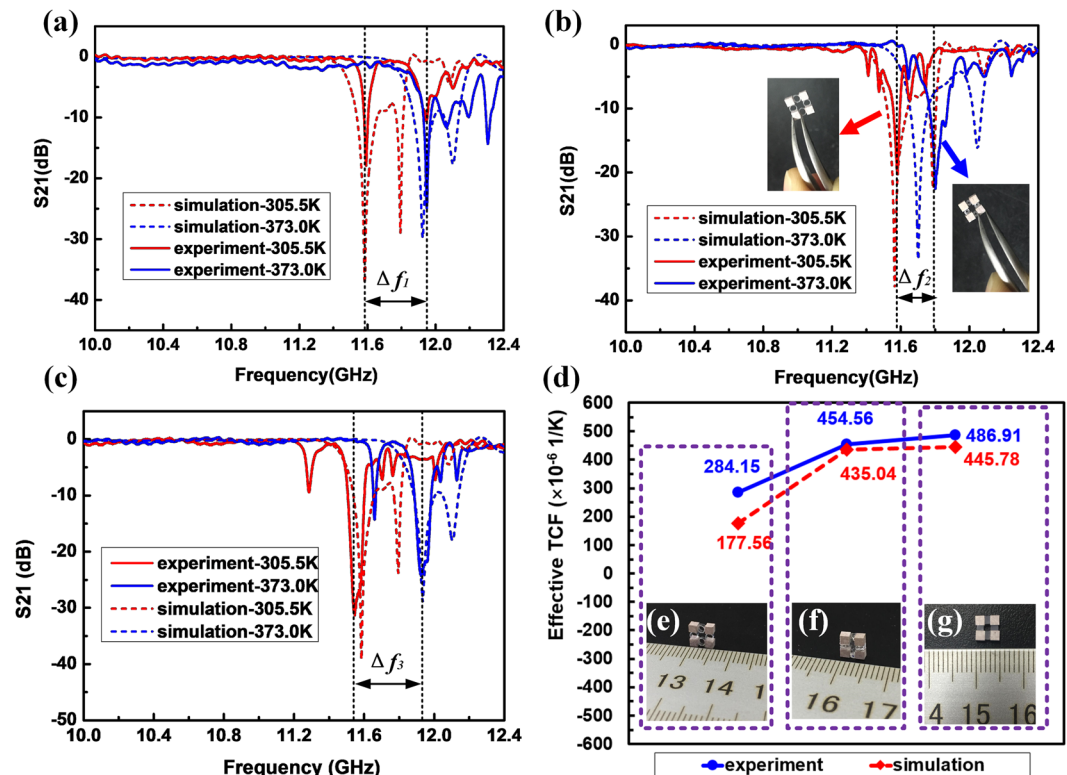
Figure 5. (**a**–**c**) The simulated and measurement resonance frequency shift of met-atom with intermediate layer of (**a**) silica. (**b**) heat-shrink tubing and (**c**) rubber. (**d**) The comparison of simulated and experiment effective TCF of the three meta-atoms. (**e**–**g**) Photos of the fabricated meta-atom samples. From left to right these are the heat shrink tubing layer, the silica layer, and the rubber layer. Photo insets in (**b**) show the initial shape (red arrow) of the meta-atom sample with heat-shrink tubing layer and its deformed shape (blue arrow) after heating.

Conclusions

In this paper, we introduced materials with widely different CTEs into an EM meta-atom to manipulate the temperature sensitivity of its resonant frequency. Both simulation and experiment show that, by appropriately designing the meta-atom and selecting the intermediate material with suitable CTE, its microwave resonance blue shift could within limits be selected. This study covered a temperature range from 305.5 K to 373.0 K. Considering future developments, artificial materials with tunable CTE could be accessible by 3D-printing process, allowing a much broader choice for the intermediate layer material. Furthermore, this method could also be applied in the Terahertz, infrared or even optical frequencies on scaled meta-atoms.

Methods

Sample preparation. The ceramic dielectric was fabricated in a solid-state reaction by mixing $CaTiO_3$ powders with $1\,wt\%ZrO_2$. The dielectric cubes were cut from a dielectric ceramic plate into dimensions of $2\,mm \times 2\,mm \times 2\,mm$. The meta-atoms were constructed by adhering the dielectric cubes with three different intermediate layers. The various fabricated meta-atom samples are shown in Fig. 5(e–g).

Simulation and measurement. The meta-atom samples were measured using two WR-90 rectangular waveguides with sectional sizes of $22.86\,mm \times 10.16\,mm \times 100\,mm$. The other ends of the two waveguides were connected to the input and output of an Agilent Technologies N5230C vector network analyzer. The S_{21} microwave transmission spectra calculations used the CST studio suite 2016 Microwave Studio software package.

Data Availability. The datasets generated during and analyzed during the current study are available from the corresponding author on reasonable request.

References

1. Zheludev, N. I. & Kivshar, Y. S. From metamaterials to metadevices. *Nat. Mater.* **11**, 917–924 (2012).
2. Smith, D. R., Pendry, J. B. & Wiltshire, M. C. K. Metamaterials and negative refractive index. *Science.* **305**, 788–792 (2004).
3. Shalaev, V. M. Optical negative-index metamaterials. *Nat. Photon.* **1**, 41–48 (2007).
4. Smith, D. R., Padilla, W. J., Vier, D. C., Nemat-Nasser, S. C. & Schultz, S. Composite medium with simultaneously negative permeability and permittivity. *Phys. Rev. Lett.* **84**, 4184–4187 (2000).
5. Pendry, J. B. Electromagnetic materials enter the negative age. *Phys. World.* **14**, 47–51 (2001).
6. Parazzoli, C. G. *et al.* Performance of a negative index of refraction lens. *Applied Physics Letters* **84**, 3232–3234 (2004).

7. Schurig, D. *et al*. Metamaterial electromagnetic cloak at microwave frequencies. *Science* **314**, 977–980 (2006).
8. Cai, W., Chettiar, U. K., Kildishev, A. V. & Shalaev, V. M. Optical cloaking with metamaterials. *Nature Photonics* **1**, 224–227 (2007).
9. Pendry, J. B., Schurig, D. & Smith, D. R. Controlling electromagnetic fields. *Science* **312**(5781), 1780–1782 (2006).
10. Pendry, J. B. Negative refraction makes a perfect lens. *Phys. Rev. Lett.* **85**, 3966–3969 (2000).
11. Fang, N., Lee, H., Sun, C. & Zhang, X. Sub-diffraction-limited optical imaging with a silver superlens. *Science.* **308**, 534–537 (2005).
12. Han, Z., Kohno, K., Fujita, H., Hirakawa, K. & Toshiyoshi, H. MEMS reconfigurable metamaterial for terahertz switchable filter and modulator. *Optics Express* **22**, 21326–21339 (2014).
13. Yang, K., Liu, S., Arezoomandan, S., Nahata, A. & Sensale-Rodriguez, B. Graphene-based tunable metamaterial terahertz filters. *Applied Physics Letters* **105** (2014).
14. Xiang, Y., Wen, S., Dai, X. & Fan, D. Modulation instability in nonlinear oppositely directed coupler with a negative-index metamaterial channel. *Physical Review E* **82** (2010).
15. Zhu, H., Yi, F. & Cubukcu, E. Plasmonic metamaterial absorber for broadband manipulation of mechanical resonances. *Nature Photonics* **10**, 709–714 (2016).
16. Zhao, Q., Zhou, J., Zhang, F. & Lippens, D. Mie resonance-based dielectric metamaterials. *Materials Today* **12**, 60–69 (2009).
17. Ghosh, I. S., Hilgers, A., Schlenker, T. & Porath, R. Ceramic microwave antennas for mobile applications. *Journal of the European Ceramic Society* **21**, 2621–2628 (2001).
18. Freer, R. Microwave Dielectric Ceramic-an Overview. *Silicates Industrials* **9**, 191–194 (1993).
19. Fuli, Z., Qian, Z., Lei, K., Ji, Z. & Lippens, D. Experimental verification of isotropic and polarization properties of high permittivity-based metamaterial. *Phys. Rev. B, Condens. Matter Mater. Phys. (USA)* **80**, 195119 (2009).
20. Zhao, Q. *et al*. Experimental Demonstration of Isotropic Negative Permeability in a Three-Dimensional Dielectric Composite. *Phys. Rev. Lett.* **101**, 027402 (2008).
21. Rachford, F., Armstead, D., Harris, V. & Vittoria, C. Simulations of Ferrite-Dielectric-Wire Composite Negative Index Materials. *Phys. Rev. Lett.* **99**, 057202 (2007).
22. Yannopapas, V. & Moroz, A. Negative refractive index metamaterials from inherently non-magnetic materials for deep infrared to terahertz frequency ranges. *J. Phys.: Condens. Matter.* **17**, 3717–3734 (2005).
23. Ueda, T., Lai, A. & Itoh, T. Demonstration of Negative Refraction in a Cutoff Parallel-Plate Waveguide Loaded with 2-D Square Lattice of Dielectric Resonators. *IEEE Trans. Microw. Theory Tech.* **55**, 1280–1287 (2007).
24. Shibuya, K. *et al.* Terahertz metamaterials composed of TiO_2 cube arrays, Proceedings of Congress on Advanced Electromagnetic *Mater. in Microw. and Opt.* 777–779 (2008).
25. Reaney, I. M. *et al.* On the temperature coefficient of resonant frequency in microwave dielectrics. *Philosophical Magazine a-Physics of Condensed Matter Structure Defects and Mechanical Properties* **81**, 501–510 (2001).
26. Lemanov, V. V., Sotnikov, A. V., Smirnova, E. P., Weihnacht, M. & Kunze, R. Perovskite $CaTiO_3$ as an incipient ferroelectric. *Solid State Commun* **110**, 611–614 (1999).
27. Kell, R. C., Green ham, A. C. & Olds, G. C. E. High-permittivity temperature-stable cermaics dielectrics with low microwave loss. *J. Am. Ceram. Soc* **56**, 352–354 (1973).
28. Cho, W. W., Kakimoto, K. I. & Ohsato, H. High-Q Microwave Dielectric $SrTiO_3$-doped $MgTiO_3$ Materials with Near-zero Temperature Coefficient of Resonant Frequency. *Jpn. J. Appl. Phys.* **43**, 6221–6224 (2004).
29. Wakino, K. Dielectric Materials for Dielectric Resonator. Japan: Joint Convention Record of Four Institute of Electrical Engineers, **235** (1976).
30. Kawashima, S. Ba (Zn, Ta) O_3 Ceramics with Low Dielectric Loss at Microwave Frequencies. *J. Am. Ceram. Soc.* **66**, 421–423 (1983).
31. Kelly, A., McCartney, L. N., Clegg, W. J. & Stearn, R. J. Controlling Thermal Expansion to Obtain Negative Expansivity Using Laminated Composites. *Compos. Sci. Technol.* **65**, 47–59 (2005).
32. Grima, J. N. *et al*. Adjustable and Negative Thermal Expansion from Multilayered Systems. *Phys. Status Solidi RRL.* **4**, 133–135 (2010).
33. Grima, J. N., Ellul, B., Gatt, R. & Attard, D. Negative Thermal Expansion from Disc, Cylindrical, and Needle Shaped Inclusions. *Phys. Status Solidi B* **10**, 2051–2056 (2013).
34. Grima, J. N., Ellul, B., Attard, D., Gatt, R. & Attard, M. Composites with Needle-like Inclusions Exhibiting Negative Thermal Expansion: A Preliminary Investigation. *Compos. Sci. Technol.* **70**, 2248–2252 (2010).
35. Landert, M., Kelly, A., Stearn, J. R. & Hine, P. J. Negative Thermal Expansion of Laminates. *J. Mater. Sci.* **39**, 3563–3567 (2004).
36. Ha, C. S., Hestekin, E., Li, J., Plesha, M. E. & Lakes, R. S. Controllable Thermal Expansion of Large Magnitude in Chiral Negative Poisson's Ratio Lattices. *Phys. Status Solidi B.* **252**, 1431–1434 (2015).
37. Wang, Q. *et al*. Lightweight Mechanical Metamaterials with Tunable Negative Thermal Expansion. *Phys. Rev. Lett.* **117**, 175901 (2016).
38. Wu, L., Li, B. & Zhou, J. Isotropic Negative Thermal Expansion Metamaterials. *ACS Appl Mater Interfaces* **8**, 17721–7 (2016).

Acknowledgements

Author Contributions

Ji Zhou conceived the idea. Lingling Wu and Xiaoqing Xi designed experiments and carried out numerical calculations. Bo Li revised the full paper. All authors contributed to scientific discussion and critical revision of the article.

Additional Information

Competing Interests: The authors declare that they have no competing interests.

Publisher's note: Springer Nature remains neutral with regard to jurisdictional claims in published maps and institutional affiliations.